

Flexural Capacity of a Cantilever RC Beam Planted on an Existing Column

Hesham Ahmed Haggag¹, Mohamed H. Agamy² and Doaa Ahmed Mohamed³

¹ Associate prof., Department of Civil Engineering, Helwan University, Elmatariah, Cairo, Egypt.

² Lecturer, Department. of Civil Engineering, Helwan University, Elmatariah, Cairo, Egypt.

³ Teaching assistant Department. of Civil Engineering, IAEMS, EMPC, Cairo, Egypt.

ABSTRACT

The study is done to investigate the flexural capacity of reinforced cantilever beam planted on existing reinforced concrete column. The study is performed in two stages. The first stage is done to evaluate the tensile capacity of single adhesive steel planted bars in concrete block and are subjected to pull-out loading. The second stage is done to assess the flexural capacity of a planted reinforced concrete cantilever on an existing column. The investigations are done experimentally, theoretically and numerically in both stages. A nonlinear finite element software (ANSYS) is utilized for the numerical analysis. In stage I: pull out tests are done on eight specimens with varying parameters like the planted bars' diameters ($d=12$ mm and 16 mm) and the embedment length ($h_{ef}=6d, 8d, 10d, \text{ and } 12d$). Additional four specimens are evaluated numerically only with additional parameters like the bar diameter ($d=10$ mm) and the effect of different configuration for fixing the specimens in the pull out testing (four configurations are investigated). All those specimens are evaluated also in according to ACI 318-14 recommendations. The results of stage I study showed that: (1) very good agreement for all the studying methods, (2) the bar diameter doesn't have a significant effect on the tensile capacity of the planted bars since they suffer concrete breakout failure, (3) using embedment length of $12d$ achieve the target capacity, (4) the specimen fixation method has influence the testing results.

In stage II: the studying parameters are the reinforcement ratio of the tensile planted bars ($\mu = 0.24\%, 0.36\%, 0.48\%, \text{ and } 0.60\%$), the embedment lengths of ($15d$ and $20d$), and the orientation of the embedded bars. Those specimens are evaluated experimentally and numerically whereas two extra specimens are evaluated numerically only. The measured factors includes the tip cantilever deflection, the strains in the planted bars, the cracks pattern, and the failure modes. The results of stage I study showed that: (1) very good agreement between the experimental and the numerical methods, (2) increasing of the embedment length of the planted steel bars from $15d$ to $20d$ has a great effect on their flexural capacities, (3) using a reinforcement ratio doubled of those for the control specimen with embedment depth of $20d$ gives the best performance with respect to the load, deflection, and ductility

Keywords: flexural capacity; planting reinforced cantilever beams; tensile capacity; ACI 318-14; ANSYS.

1 INTRODUCTION

In existing reinforced concrete buildings, their interior design may be changed in according to the purpose of the buildings use. Some additional cantilever beams may be required to create an extension of the building. The subject of our study investigates the efficiency of planting a reinforced concrete cantilever beam on an existing RC column. The flexural capacity and the deflection of those beams are studied. The planting is done using chemical adhesive material with different embedment lengths, bar diameters, and reinforcement ratios at the planted section.

2 LITERATURE REVIEW

In general the planting elements is fabricated using anchored steel bars. Those anchors may be manufactured using different methods such as mechanical, or chemical. The efficiency of that type of connection is influenced by many factors. Factors may affect the bond strength of the adhesive anchors and the modes of failure are presented below as found in the literature of the subject.

2.1 Adhesive Material

There are many factors may affected on the adhesive efficiency as:

- Type of adhesive:** Cook and Konz (2001) [4] noticed that the adhesives can vary significantly in the bond strength for chemical groups and even within chemical groups.
- Mixing methodology:** Manufacturers recommend mixing until a certain consistency and color is reached. The adhesive must completely fill any voids between the anchor and the holes because the voids will decrease the effective area and subsequently the bond stress.
- Adhesive curing time during first loading:** According to Cook and Konz (2001) [4], the bond strength of the anchor decreases with a shorter adhesive cure time and the average bond strength for a 24 hour cure achieve 88% of ones with seven day curing.
- Bond line thickness:** According to Çolak (2007) [3], the smaller space between the anchor and the side of the hole has higher potential for creep occurrence.

2.2 Surface Preparation and Bars Installation

As well, there were several factors have affected on the preparation of the installation of anchors as presented below:

- a) **Hole orientation:** ACI 318-14 [1] requires that the installation of adhesive anchors horizontally or upwardly or inclined to sustained tensile loads shall be performed by a certified personnel.
- b) **Hole drilling** Methods of drilling the hole were rotary hammer, core drill, or drilled in accordance with manufacturer's instructions have the potential to significantly affect the performance of the strength of the adhesive anchors.
- c) **Hole cleaning:** As required by ACI 318-14 [1], the hole cleaning is intended to ensure that drilling debris and dust do impair the bond efficiency. Brushing has a significant effect on the cohesion efficiency. FDOT [6], recommends cleaning the holes with a non-metallic brush.
- d) **Moisture in installation:** It was demonstrated by Cook and Konz [4], that the dampness of the hole has a significant effect of the bond strength, the moisture can interfere with the chemical reaction between the hardener and the adhesive material.
- e) **Embedment depth (h_{ef}):** Krishnamurthy [7], the load increases proportionally up till $h_{ef} = 25d$ and then drops. According to ACI 318-14 [1], the maximum embedment depth shall be 20 d.
- f) **Type of concrete:** Cook and Konz (2001) [4], there was no broad rules can be applied between bond strength and concrete strength among the adhesives tested.
- g) **Anchors spacing,** Siamak and Omid [8], the tensile failure mode of a single anchors may be a steel-fracture or concrete breakout or a bond failure. Also, a group of anchors may face concrete cone splitting failure. The spacing between anchors influence the tensile capacity.

2.3 Modes of Failure

According to Blaz Zoubek [2], there are two types of failures: local failure and global failure. The connections are subjected to the following types of potential failure mechanism: local failure characterized by the yielding of the dowel and crushing of the surrounding concrete, and global failure, characterized by spalling of the concrete between the dowel and the edge of the concrete elements. According to ACI 318-14 [1] failure modes for anchors under tension forces are steel failure of anchor in tension or concrete breakout or bond failure of the adhesive surface.

3 STUDYING PROGRAM

The studying program is divided into two stages. Stage I: investigate small specimens with steel bars planted in concrete blocks. Pull out test is done on those specimens. Stage II: investigate reinforced concrete cantilevers planted on existing columns. Point load at the tip of each cantilever specimen is applied on those specimens to investigate their flexural capacities. Every stage is studied experimentally and numerically. The results of each stage are presented and compared. A conclusion is deduced to be used as a guidelines for the design of such case. In addition, the calculated values from ACI equation are compared.

4 PHYSICAL PROPERTIES OF THE USED MATERIALS

Concrete material: normal weight concrete is prepared using a tilting drum mixer. The compressive strength is 26 MPa after 28 days with a maximum aggregate size of 20 mm.

Steel reinforcement: High strength of deformed bars with yield strength of 40 MPa were used as main reinforcement. Mild strength steel bars are used for stirrups in specimens. The clear concrete cover is 25 mm to the outside of stirrups for all reinforced specimens. The average yield and ultimate strengths of the tested bars ($d=12, 16$ mm) are 351 and 540 N/mm², respectively.

Adhesive material: Sikadur-31CF (normal type) is utilized. It is a solvent-free, thixotropic, two components (A&B) adhesive and repair mortar, based on a combination of epoxy resins, and selected high strength fillers. The mechanical properties of such material is shown in Table 1.

Table 1: Mechanical properties of Sikadur-31CF, normal type.

Compressive strength		Flexural strength	30-40 N/mm ²
After 24 hours at +20°C	60-70 N/mm ²	Tensile strength	15-20 N/mm ²
After 24 hours at +30°C	40-45 N/mm ²	Bond strength to concrete	3.5 N/mm ²
After 24 hours at +50°C	35-40 N/mm ²	Bond strength to steel	15 N/mm ²
Thermal Expansion Coeff.	5.9×10^{-5} per °C	Elastic modulus	4.6-5.0 KN/mm ²

5 STAGE I: PULL OUT TESTING

The main objective of this stage is done on existing eight concrete prismatic blocks with dimensions of 250x250x500 mm. Steel bars with variable diameters and embedment lengths are fixed into those blocks after 28 days of casting using the above mention adhesive material. The variable parameters are the bar diameters and the embedment length values. Bars with a diameters of 12 and 16 mm are utilized. Also, embedment lengths of 6, 8, 10 and 12 of the bar diameters (d) are used. Pullout test is done on all specimens. Those specimens are investigated experimentally and numerically. In addition extra specimens are investigated numerically only. Table 2 shows the specimens configuration with the changing parameters.

5.1 Test Setup

A hole is done at the center of the top face of each specimen. The hole has a diameter larger than the planted bars by 2 mm. The hole is cleaned well with compressed air. The above specified epoxy material is injected in the holes and a testing bar is driven into the hole. The concrete block specimen was placed in the tensile testing machine as shown in Figure 1. Each specimen is fixed into the machine jaw through a steel plate underneath the specimen and two angles placed atop of them. The upper Jaw clamped on the steel bars and pulled it till failure.



Figure 1: Test setup for stage I.

5.2 Crack Pattern and Mode of Failure

The cracks developed in all tested specimens are almost in similar pattern. The failure shaped a concrete breakout cone. No bar slippage is found in all specimens. The failure is found in the concrete part only. Figure 2 shows the crack pattern for each specimens as titled in Table 2.

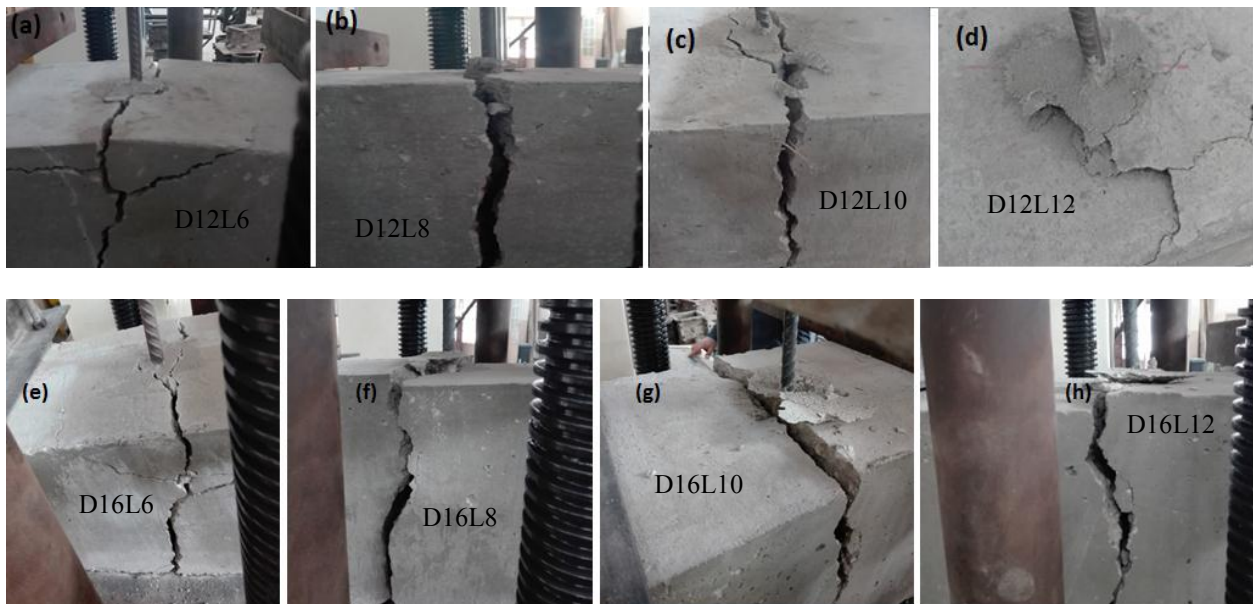


Figure 2: Modes of failure of pullout tested specimens.

5.3 Failure Loads

The failure load for each specimen is presented in Table 2. It is found that the embedment length has a significant effect on the capacity of the planted steel bars connection. With the same

embedment length, the bar diameter has a slightly effect on changing the capacity of the embedded steel bars connection, as seen in Table 2.

Table 2: The results of the tested specimens in the stage I.

Name	d (mm)	hef (mm)		P _{EXP} (KN)	P _{ACI} (KN)	P _{ANSYS} (KN)	P _{EXP./} p _{ACI}	P _{EXP./} P _{ANSYS}	P _{ANSYS/} p _{ACI}
D12L6	12	6d	75	30.8	24.8	26	1.24	1.18	1.05
D12L8		8d	100	36.3	32.7	34	1.11	1.07	1.04
D12L10		10d	120	45.2	41.1	43	1.10	1.05	1.05
D12L12		12d	145	60.3	52.4	56	1.15	1.08	1.07
D16L6	16	6d	100	42	32.7	34	1.28	1.24	1.04
D16L8		8d	125	49.6	43.3	46	1.15	1.08	1.06
D16L10		10d	160	65.4	59.7	63	1.10	1.04	1.06
D16L12		12d	195	85.3	77.7	82	1.10	1.04	1.06
D10L20	10	20d	200	--	80.35	84	--	--	1.05
D12L10A	12	10d	120	--	41.1	49	--	--	--
D12L10B				--		58	--	--	--
D12L10C P				--		58	--	--	--

“D12” means using steel bar with 12mm in diameter and “L6” means using steel bar with an embedment length equal to 6d in the concrete block. Where d is the bar diameter. Models, D12L10A, B, C has different configuration for fixing the specimens as shown in figure 3. The dashed cells indicate that the specimens are investigated numerically only.

5.4 Calculation of the Failure Loads using ACI 318-14 Specifications

The expected failure load is calculated by applying ACI 318-14 equations as shown in equation numbered 17.4.2.1a for single anchor in that specification. Equation 1 shows that equation where the notations are defined in specifications. You may consider the value of N_{cb} as the maximum load for its specified anchor. That equation considers the anchor length, the bar diameter, the bar location, and the concrete strength. The vales are presented in Table 2 with a comparison with the experimental results. Where: N_{cb} = the basic concrete breakout strength of a single anchor in tension in cracked concrete., $\Psi_{ed,N}$ = the modification factor for the edge effects for single anchors or anchor groups loaded in tension, $\Psi_{c,N}$ = modification factor based on presence or absence of cracking, and $\Psi_{cp,N}$ = modification factor for post-installed anchors designed for uncracked concrete without supplementary reinforcement to control splitting.

$$N_{cb} = \frac{A_{Nc}}{A_{Nco}} \Psi_{ed,N} \Psi_{c,N} \Psi_{cp,N} N_b \quad \text{Equation 1}$$

This comparison demonstrates that the experimental capacity load is close to the ACI predicted values but it is higher than that of codes equations.

5.5 Numerical Investigation for the Pullout Specimens

A finite element model is built using ANSYS 19, general purpose finite element program, to investigate the failure loads for such specimens. Also, the cracking pattern and mode of failure. The model is shown in Figure 3. SOLID65, LINK180,

are used for solid concrete elements and for the steel bars consequently. All the properties for the used material are considered in the model. SOLID65 element has eight nodes with three degrees of freedom at each node and translations in the nodal x, y, and z directions. This element represents cracking in three orthogonal directions, crushing, plastic deformation, and creep for the concrete material. LINK180 is used to model the reinforcement material in most of the studies reviewed if it is in the form of rebar or tendon. In addition, SOLID185 is used for 3-D modeling of solid structures. It is defined by eight nodes having three degrees of freedom at each node: translations in the nodal x, y, and z directions. This element has plasticity, stress stiffening, creep, large deflection, and large strain capabilities. It has mixed formulation capability for simulating deformations of nearly incompressible elastoplastic materials, and it is used to model the support plates and the loading to avoid stress concentration. The bars are tensioned till failure.

Additional models are investigated for the method of restraining the top surface of the specimens. That is done for specimens D12L10A, D12L10B, D12L10 C, where the location of the constrain parts at the top surfaces is changed as shown in figure 3. The ultimate loads are found for each specimens and presented in table 2. The unltimate loads are incresed with moving the constrain parts at the top surface towards the planted bar. The first model with a relative distance between the constrain plates are 500 mm achieved an ultimate loads close to the experimental findings. Thoigh, the models done for the rest of the specimens are reliable.

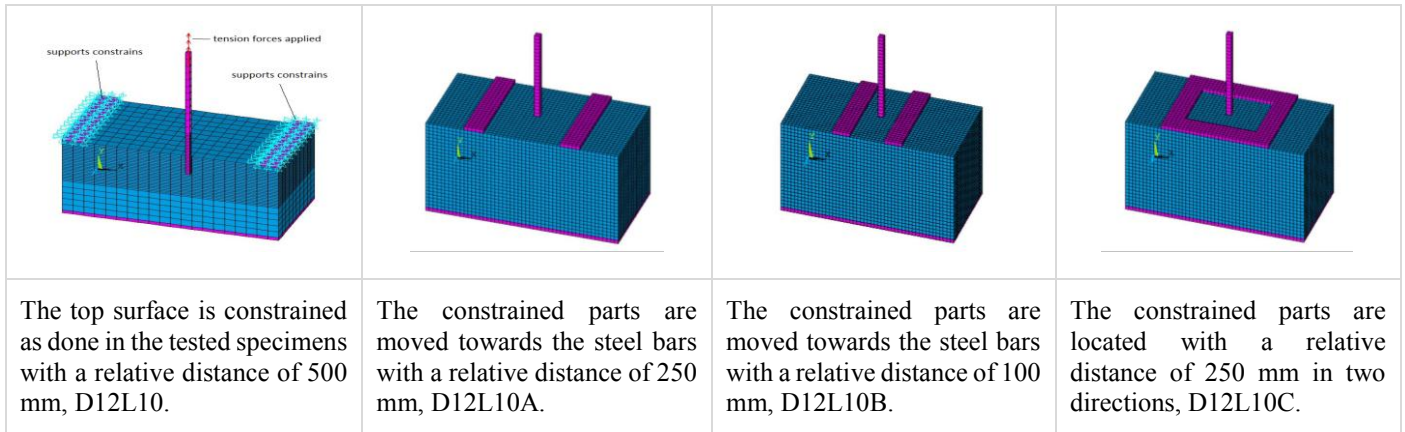


Figure 3: Numerical models for the pull-out specimens with different configuration of the constrain locations at the top surfaces of the specimens.

5.5.1. Cracking pattern and modes of failure

It is found that the failure type for all specimens is breakout failure. The shape of failure in ANSYS model was close to the experimental pattern. The values of the calculated failure load are organized in Table 2. Additional models is done for bar diameter of 10 mm which is presented in that table and compared with the ACI values. The cracking behavior at

failure stage as recorded from the ANSYS pullout models is displayed in Figure 4 for some specimens. The cracking shape for all modeled specimens experienced similar contour to their corresponding experimental models. Also, those cracks were followed by concrete breakout failure with the cone shape. In addition, that cone shape has an inclination angle of ~ 35 degrees as mentioned in ACI318-14 [1].

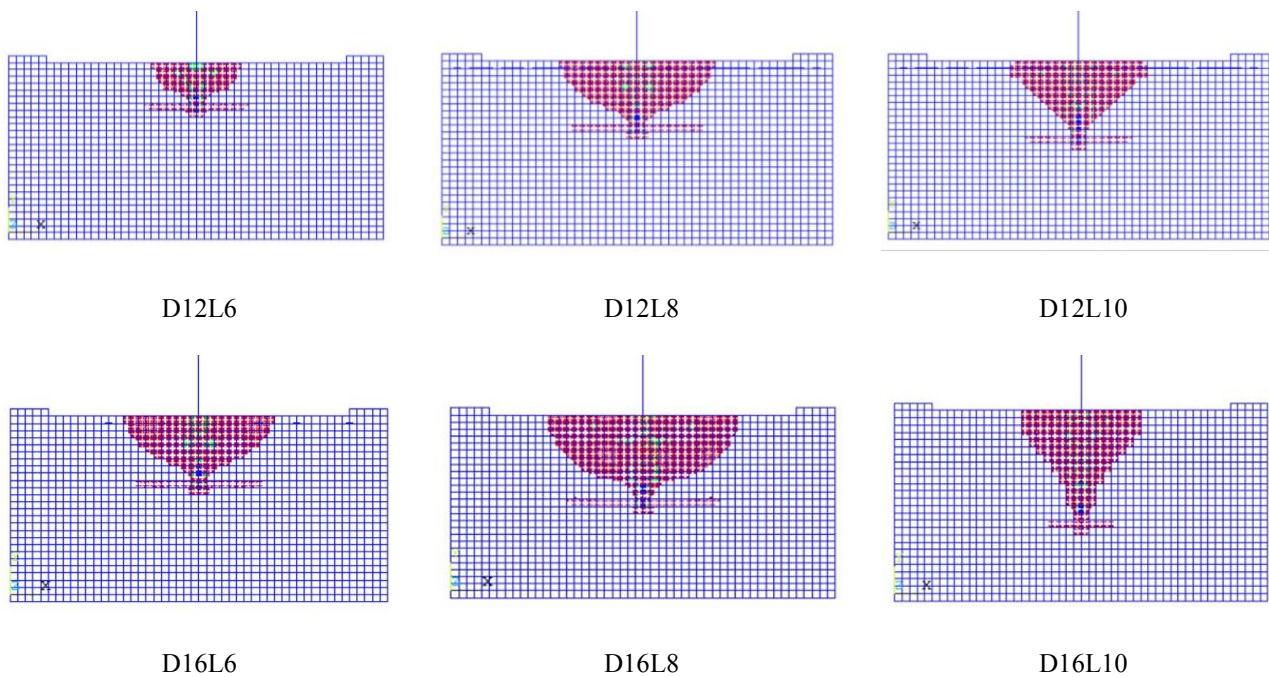


Figure 4: Crack patterns for some of the modeled specimens.

Figure 5 showed the concrete stresses at section through the planted steel bar showing principal stress contour. The general concrete stress for all the pull-out models is relatively similar to the stress pattern shape but it is changed with increasing the embedment length of the planted steel bars as mention in

ACI318-14 as shown in figure 4. The stresses are concentrated around the steel bar. The maximum concrete stress around the end of the bars achieved ~ 16 N/mm².

5.6 Analysis of the Pullout Results

The results of the failure loads as found in the experimental, ACI, and ANSYS studies are presented in figure 6 for the issue of a comparison. However the results are in good agreements

for all studies, but the experimental findings recorded the highest values for each embedment length. It is found that the increase in the embedment length as a ratio of the bar diameter increases the failure loads. In addition, the yielding loads of the planted bars are indicated on the figure.

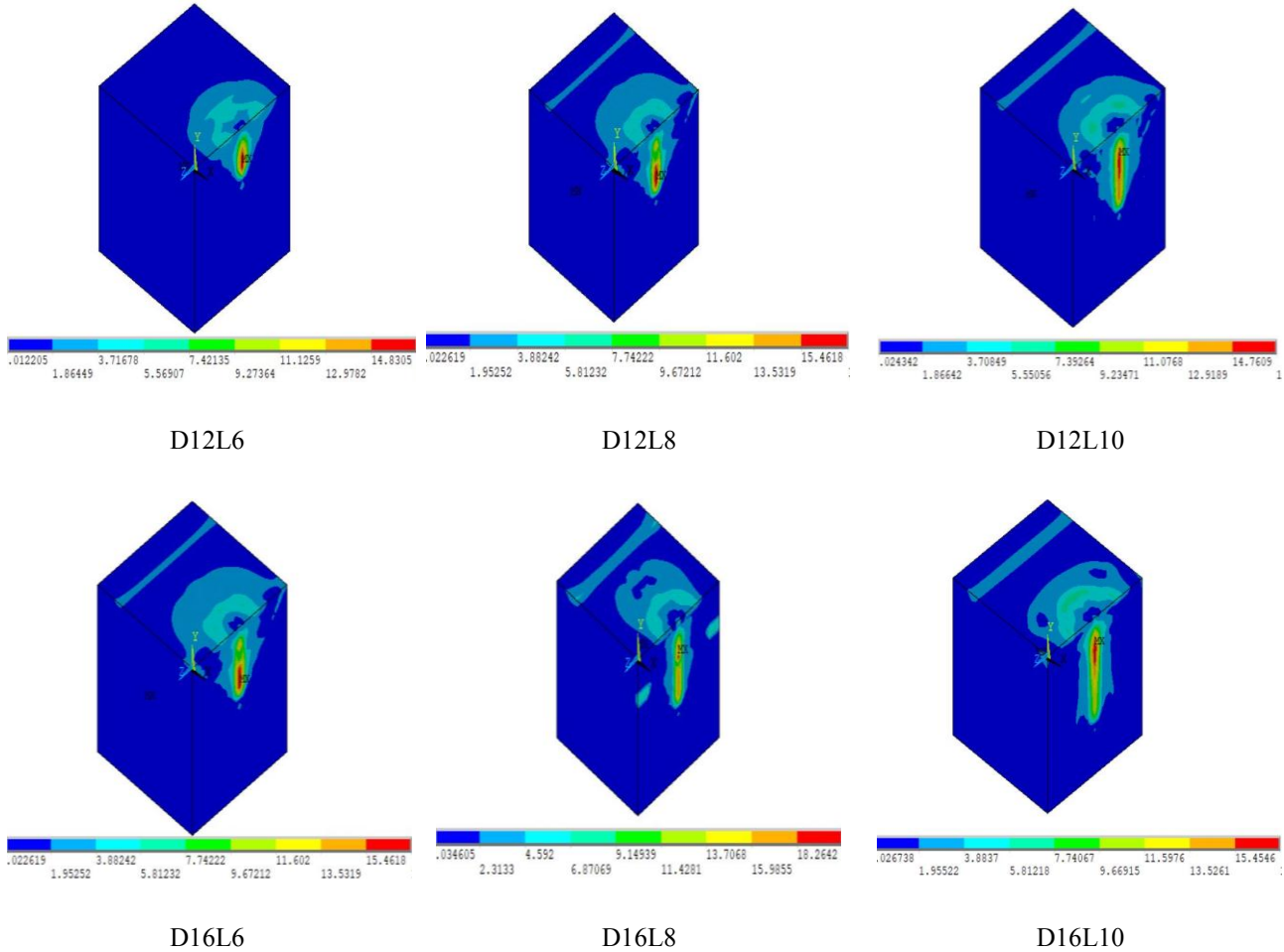


Figure 5: Stress distribution around the anchor bars.

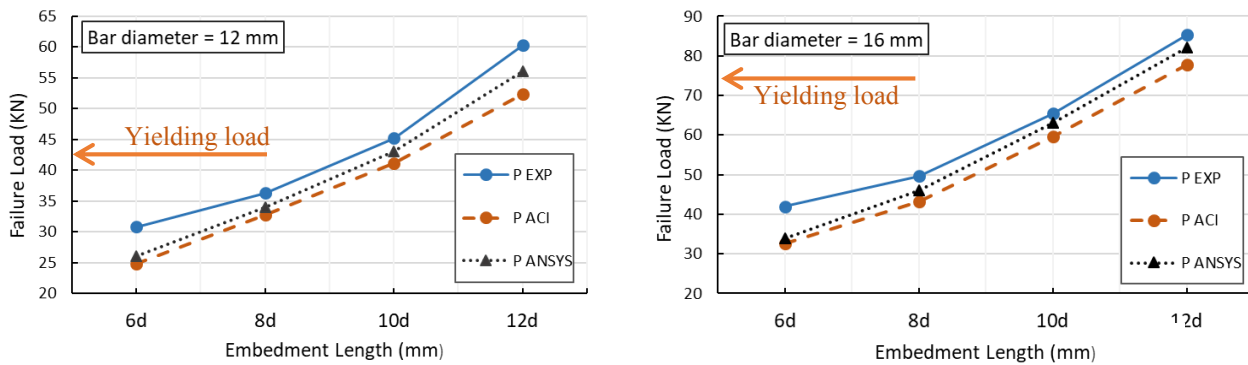


Figure 6: Failure loads for planted bars of diameter 12 and 16 mm with different embedment lengths as found from the experimental, ACI, ANSYS results

6 STAGE II: PLANTED CANTILEVER

In this stage, the efficiency of planting an RC cantilever beam on an existing column is investigated. A control specimen is built where the cantilever is casted monolithically with the column. Five configurations of the planted bars are set for planting the cantilever beam. Those specimens are investigated experimentally, and numerically. The specimen's details and the studying investigation are explained below.

6.1 Specimens Details

Five RC frames are casted to represent the existing structural case. A frame with a cantilever is built to represent the control specimen. The columns have cross section dimension of 250 x 400 mm and 1050 mm in height. The columns are reinforced with 4T10 bars. The used stirrups are R8 placed every 150 mm.

The starting and ending stirrups are placed at 100 mm from the column bottom and top levels consequently. The control cantilever specimen has a cross sectional dimension of 250 x 300 mm and length of 800 mm. It is reinforced with top and bottom reinforcement of 2 T10. The top reinforcement is extended to 1.5 times the cantilever length. All cantilever specimens are designed to fail in flexure.

Five RC cantilever beams with the same dimension as the for the control specimen are planted to the existing RC columns. Several parameters are considered for those specimens such as the number of planted bars, the embedment depth of the planted bars, and the location and orientation of the planted bars. The concrete contact surface is prepared as well as the drilled holes. The above prescribed adhesive material is used for planting the reinforcement bars. Figures 7, 8, 9 show the details of the tested specimens.

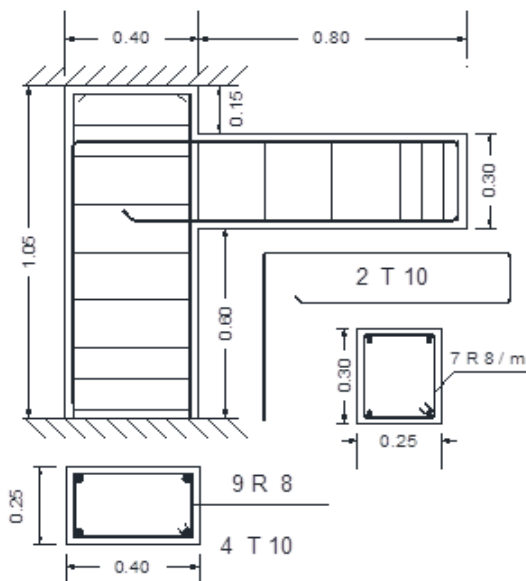


Figure 7: Details of the control specimen

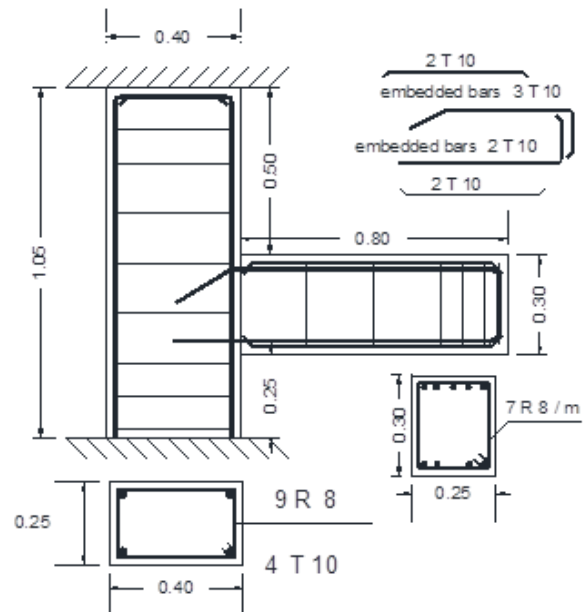


Figure 8: Details of the specimens with inclined planted bars of 3T10

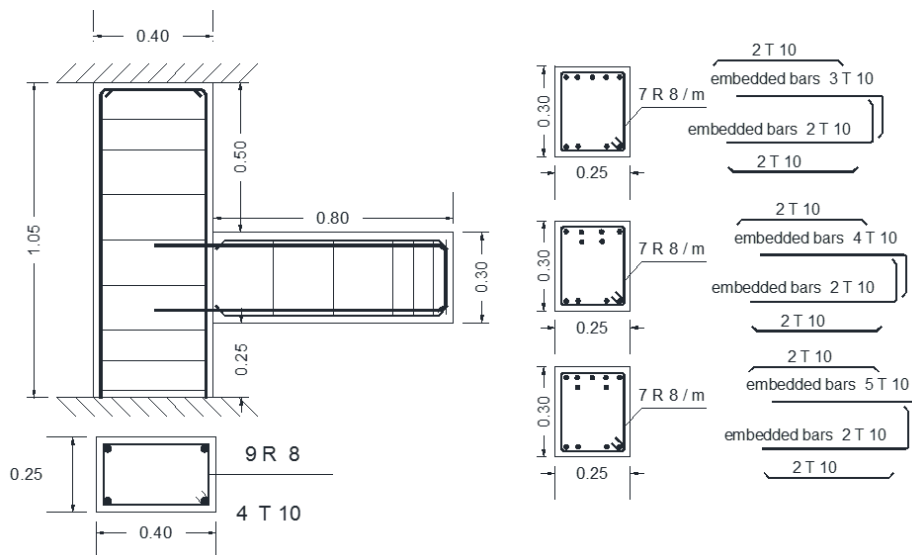


Figure 9: Details of the specimens with planted bars of 3T10, 4T10 and 5T10.

Also, Table 3 shows the details of the reinforcement for the tested specimens. For all planted cantilever beams, the spacing between the embedded steel bars center to center is 6d (60 mm) whereas the edge distance is 6d (60 mm) to prevent splitting of the surrounding concrete as recommended by ACI-318-14 [1], “the minimum edge distance shall not be less than 6d for

adhesive anchors” and “minimum center-to-center spacing of anchors shall be 6d for post-installed anchors”. In all planted cantilever beams, the upper and lower steel reinforcement of 2T10 stay at the face of the column to represent the design reinforcement of the new cantilever.

Table 3: Configuration of the tested specimens in the stage II.

Specimen	Reinforcement		Planted bars		Embedment Length		bars orientation
	Top	Bottom	Top	Bottom	# d	mm	
Control	2T10	2T10	--	--	--	--	straight
T3L20S	2T10	2T10	3T10	2T10	20 d	200	straight
T4L20S	2T10	2T10	4T10	2T10	20 d	200	straight
T5L20S	2T10	2T10	5T10	2T10	20 d	200	straight
T3L15S	2T10	2T10	3T10	2T10	15 d	150	straight
T3L20I	2T10	2T10	3T10	2T10	15 d	150	inclined

“T3” refers to planted cantilever beam with 3 planted bars, “L20” refers to steel bars planted with an embedment length of 200 mm in the column, “S” refers to straight steel bars planted without any inclination and “I” refers to planted steel bars with an inclination angle 35° from the horizontal line.

6.2 Preparation and Installation

The method of preparing the holes in stage II is presented in the following steps as shown in figure 10:

- The concrete surface was fully cured during the three weeks after pouring, and then the concrete surface was cleaned out using small wire brushes to remove all impurities and make sure that the surface is free from dust and all loosely adhering particles.
- The concrete surfaces were grounded by a rotary hammer drill and manually hammer to uncover the coarse aggregates.
- The holes were done with diameter of 15mm and cleaned by a compressed air.
- The resin material used in fixing the dowels was Sikadur-31CF, and it was mixed in according to the instruction of the manufacture.
- The mixed adhesive material was inserted in the holes manually using spatula and gloves.
- The dowels were inserted in spiral motions into the drilled holes, the excess material of Sikadur 31-CF raised up, the surplus resin was removed from the concrete surface, and it was finished to a smooth texture by hand.

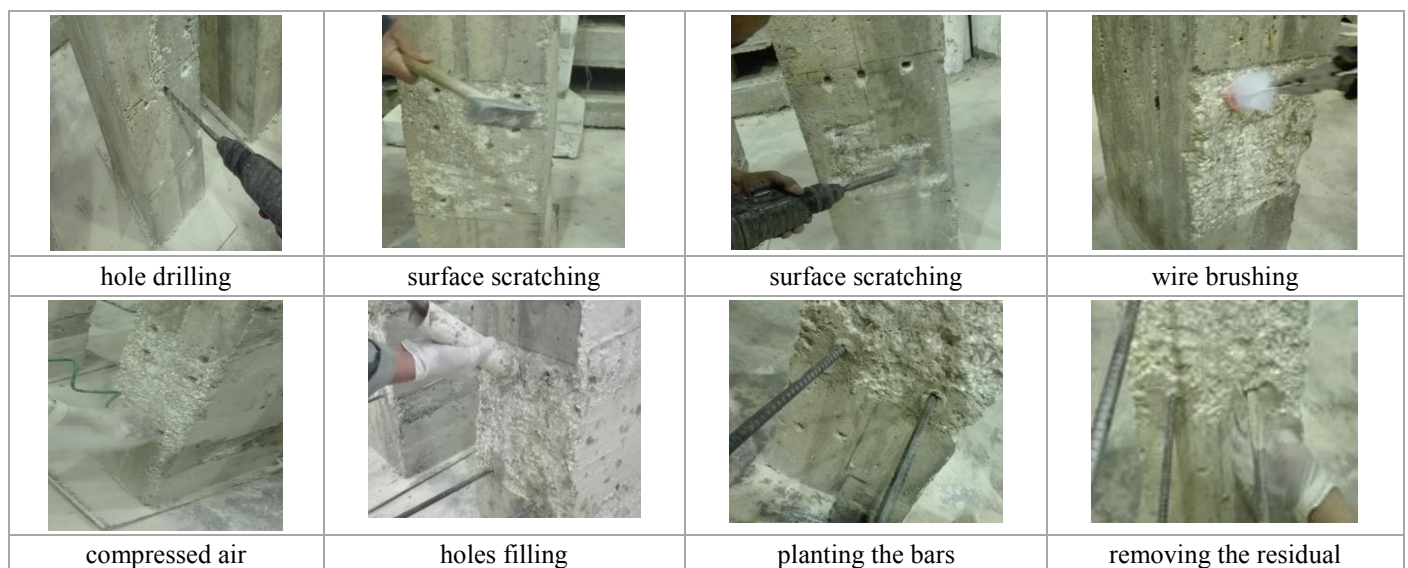


Figure 10: Preparation for installation of the planted cantilever

6.3 Test Setup and Instrumentations

A hydraulic jack with 1000 KN capacity was used to test all specimens, and it is manually operated by an oil pump. An electrical load cell with accuracy 0.1 KN connected to a digital load indicator was used to measure the applied vertical loads. The deflections of the cantilever beams were recorded by using three electrical LVDT's, the locations of those electrical LVDT's were: one at the end span of the cantilever, one at the one-third of the cantilever span and the last one was placed at the two-thirds of the cantilever span. The column were fixed

at their ends Top and bottom parts) by using anchors connected to a rigid steel frame to preclude any rotation of the columns. The load cell was used to apply the load on the specimens. Strains in the main steel, the stirrup nearby the column are measured. In addition, the strain at the concrete surfaces were measured by using electrical strain gauges in each specimen. The load cell, LVDT's and strain gauges were connected to a data acquisition system to record their measurements. Each tested specimen is loaded up till failure. The test setup and the instrumentation are shown in Figure 11.

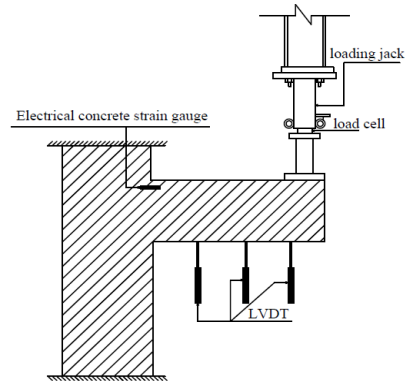


Figure 11: Test setup for stage II

6.4 Experimental Results

6.4.1. Loads at failure

The maximum loads and the failure deflection is recorded for each specimens. It is found that all specimens achieved the required loads except the last one where the bars are implemented in inclined direction. The member capacity is attained by planting the bars with embedment length of 20 d and with number of bars higher than the flexural required

reinforcement for design issue. However the flexural load is recovered for the tested specimens but their deflections are higher than the control specimens. Table 4 shows the values of the maximum loads and the deflection at maximum loads and at failure. You may notice that the bar inclination doesn't achieve the required flexural loads for the control specimen. Also, it has observed that the cracking loads are almost the same in all specimens.

Table 4: The results of the tested specimens found in the stage II study.

Specimen	Planted bars		Cracked loads (KN)	Maximum load (KN)	$P_{max} / P_{control}$	Tip Defl. at P_{max} (control) (mm)	Tip Defl. at failure (mm)
	Top	Bottom					
Control	--	--	19.53	46.53	1.00	10.42	20.36
T3L20S	3T10	2T10	25.45	63.35	1.36	8.30	24.58
T4L20S	4T10	2T10	27.15	73.03	1.56	6.50	23.90
T5L20S	5T10	2T10	31.85	76.25	1.64	4.60	23.10
T3L15S	3T10	2T10	24.85	51.85	1.11	9.20	20.25
T3L20I	3T10	2T10	18.45	33.95	0.73	--	11.60

6.4.2. Cracking pattern and modes of failure

Approximately all specimens have almost the same cracking pattern and failed with concrete breakout strength. Generally, there were two phases after the first flexural crack occurred in the column-cantilever connection, In the first phase the

cracking formation was created in the column over a triangle shape with a breakout prism angle of approximately 35 degrees, although in the second phase, the existed cracks have widened and appearing of simple cracks in the cantilever until reaching flexural failure as seen in Figure 12. The maximum failure load (P_{max}) is presente in Table 4.

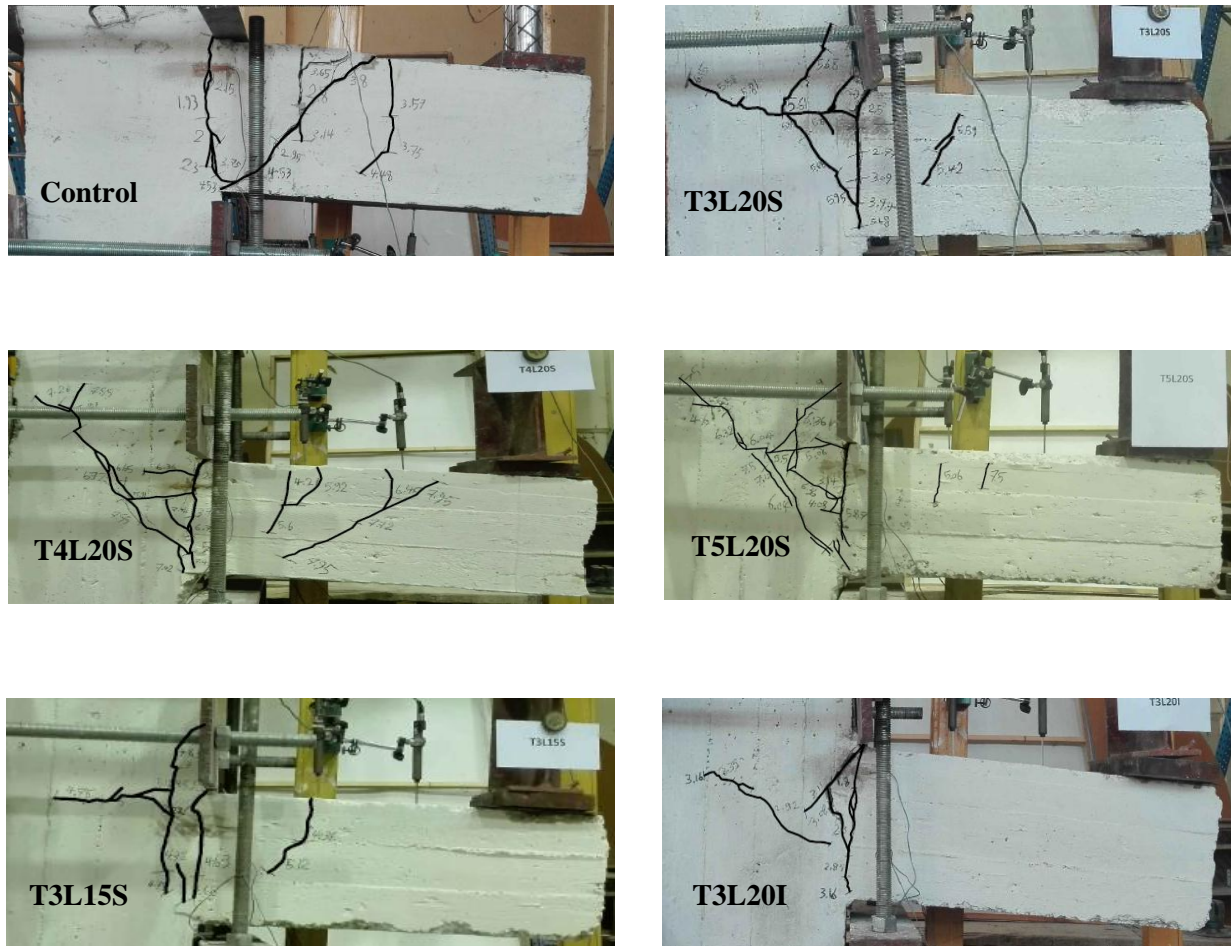


Figure 12: Modes of failure for phase II specimens.

6.4.3. Load-deflection relationship

The load-deflection curves have measured at the free end of the cantilever beam and they are indicated in Figures 13, 14, 15. As seen in Table 4, increasing of the reinforcement ratio by 0.38%, 0.5% and 0.63% was not changing the cracking load but in contrary, increases the maximum load by 36%, 73% and 64% respectively compared to the control specimen. Also, it can be concluded that using embedment length 15d and 20d with 0.38% reinforcement ratio increased the maximum load by 11% and 36% respectively compared to the control specimen, and have not a significant effect on the cracking load. It was found that the energy absorption (area under load-deflection

curves) increased by increasing the reinforcement ratio. The absorbed energy in specimen using embedment length 15d was almost equal to the control specimen but in specimen using embedment length 20d was more than the control specimen by 39%.

The initial stiffness of the control specimen was very large compared to the planted cantilever beams, and it seems that increasing the embedment length of the steel bars did not change the initial stiffness of the specimen, but increasing the reinforcement ratio increased the initial stiffness by a small rate, therefore, it is recommended to plant cantilever beam with dimensions more than the control specimen.

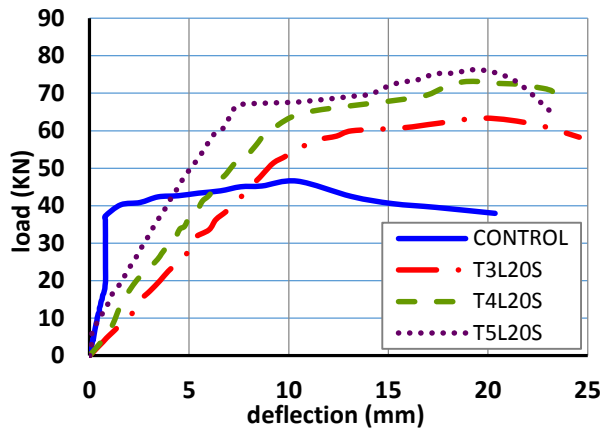


Figure 13: Load deflection relation for different numbers of the planted bars

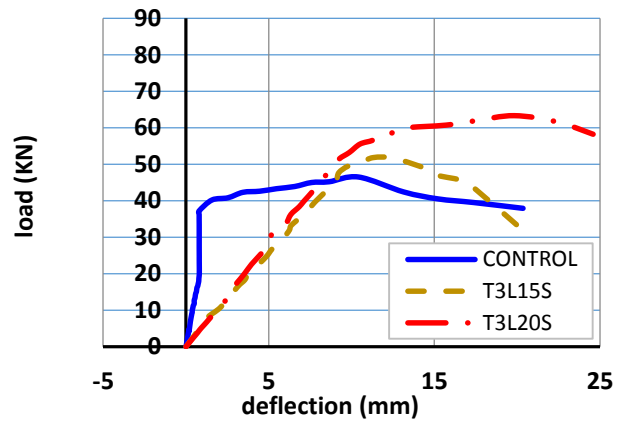


Figure 14: Load deflection relation for different embedment length of the planted bars

6.4.4. Load-Strain Relations

The load-strain of the tension planted bars curves are shown in Figure 16. In general, increasing the reinforcement ratio and

the embedment length of the planted steel bars increases the strain of the main steel bars with small rate at the same loading.

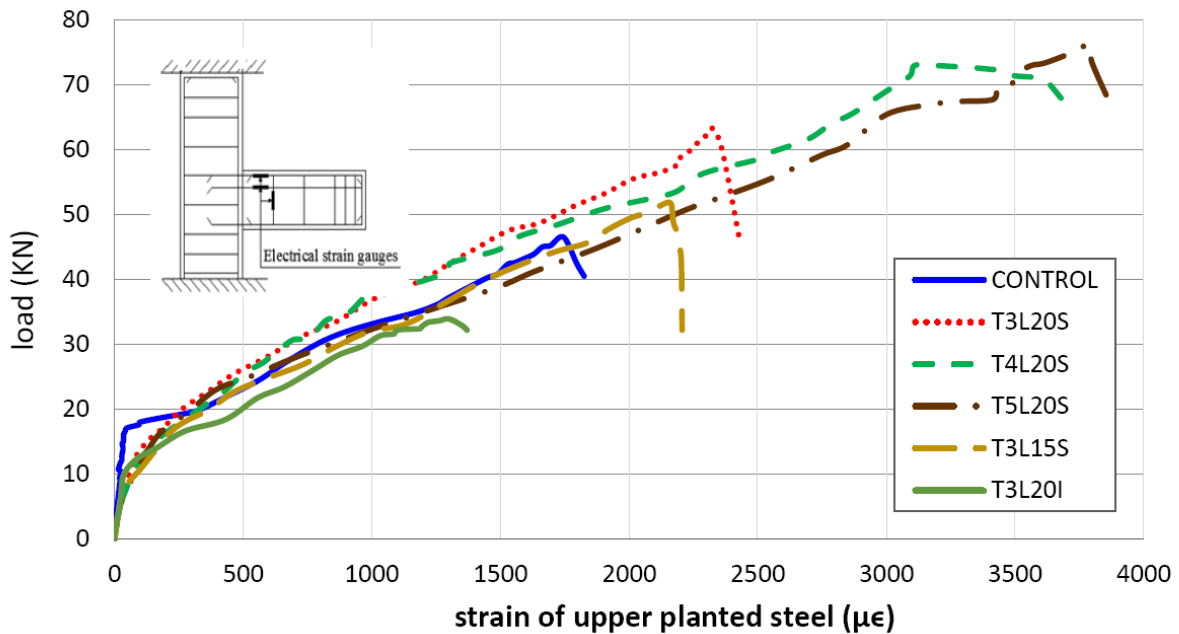


Figure 16: Strains in the planted bars at the top of the cantilever-beam connection

6.5 Numerical Evaluation of the Planted Cantilever Model

A finite element model is built using ANSYS 19, as described for Stage 1 of that research in order to investigate the failure flexural loads for such specimens. Also, the cracking pattern and mode of failure are found. The model is shown in Figure 17. SOLID 65, LINK 180, are used for solid concrete elements and for the steel bars consequently. All the properties for the used material as shown above are considered in the model.

Also, SOLID 185 is a solid element used for steel plates. The specimens are loaded till failure. Comparisons are done between the numerical findings and the experimental results.

SOLID 65 has eight nodes with three degrees of freedom at each node and translations in the nodal x, y, and z directions. This element represents cracking in three orthogonal directions, crushing, plastic deformation, and creep. Also, the element allows the presence of four different materials within each element, one matrix material (e.g. concrete) and a maximum of

three-smearred rebar. Moreover, LINK180 is a 3-D spar that is useful in a variety of engineering applications. This 3-D spar element is a uniaxial tension-compression element with three degrees of freedom at each node. SOLID185 is defined by eight nodes having three degrees of freedom at each node:

translations in the nodal x, y, and z directions. It has mixed formulation capability for simulating deformations of nearly incompressible elastoplastic materials, and it is used to model the support plates and the loading to avoid stress concentration.

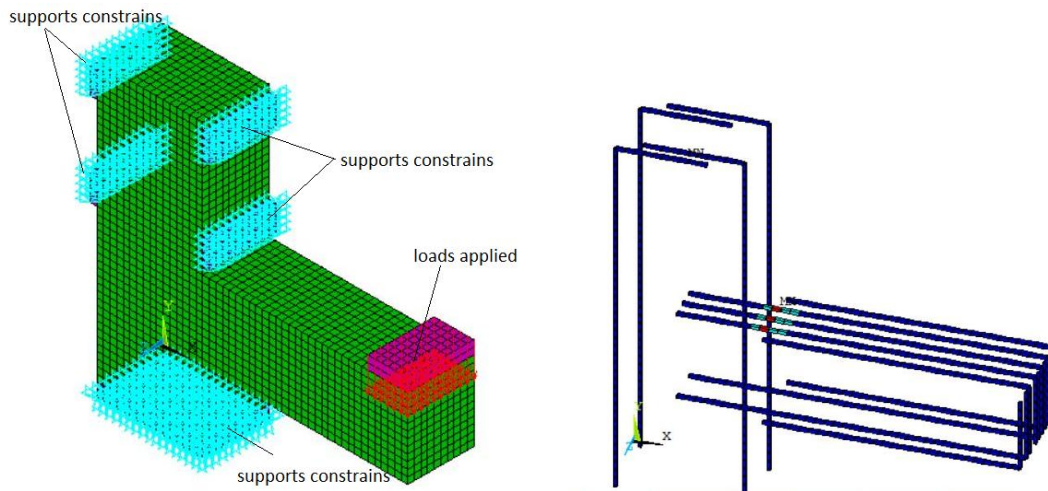


Figure 17: Element models in ANSYS for the planted cantilever beam

For the planted cantilever beams, comparisons between ANSYS and experimental results were done with respect to load-deflection relationship, load-strain of the main steel at the planted sections, failure loads, and cracks patterns at failure as shown in Figures 18 and 19.

6.5.1. Cracking pattern and modes of failure from the numerical model

The obtained cracks pattern are recorded from the ANSYS models at several stages of loadings. All specimens have almost the same cracking pattern and failed with concrete breakout. The first flexural crack occurred at the column-cantilever connection. The existed cracks in the cantilever part are widened until reaching the failure stage. The crack pattern

is presented for the control specimen in figure 18 at the failure load (46 KN). In addition, the cracks pattern are graphed for all specimens at the maximum load for the control specimens (46 KN) and at their failure loads. Those are presented in figure 19. One may notice that the crack pattern at load 45 KN does not extend in the column. Cracks at failure outspread towards the cantilever part. All cracks showed that the cohesion part works well. Better performance is found for specimens with increased the number of planted bars and also with depth of 20d.

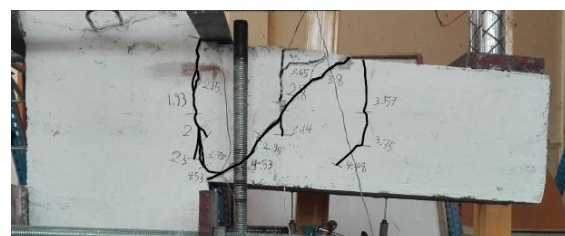
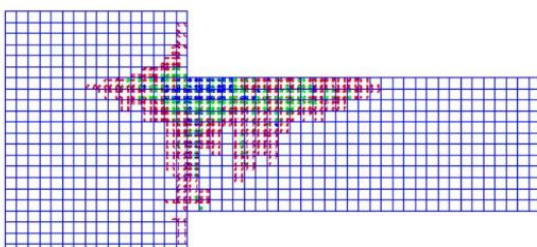


Figure 18: Cracks Pattern at failure load as obtained from the ANSYS models for the control beam in compared with the experimental findings.

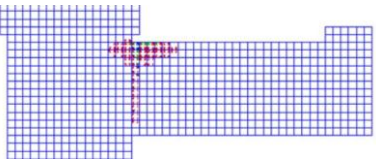
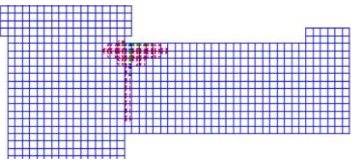
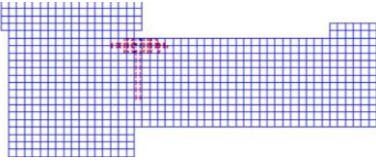
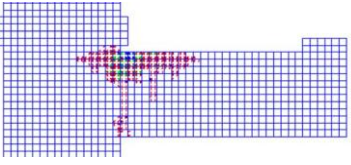
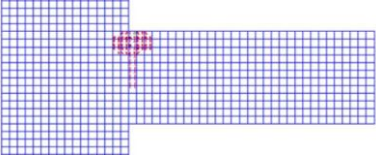
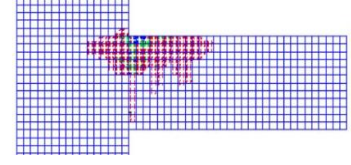
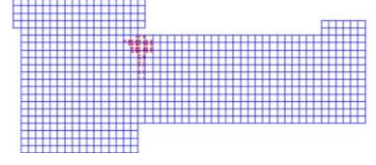
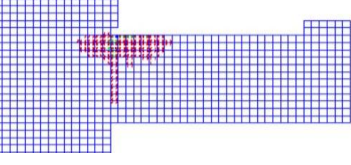
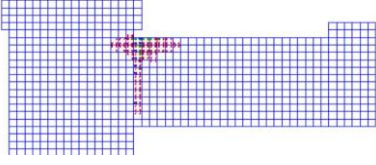
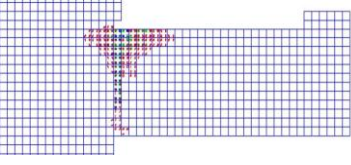
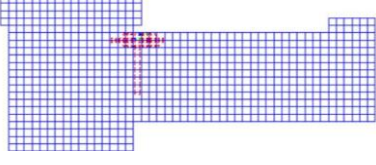
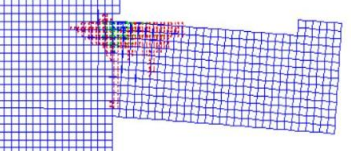
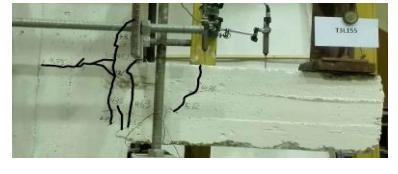
		Numerically Investigated only
T2L20S at P=46KN (ANSYS)	T2L20S at failure (ANSYS)	
		
T3L20S at P=46KN (ANSYS)	T3L20S at failure (ANSYS)	T3L20S at failure (Exp)
		
T4L20S at P=46KN (ANSYS)	T4L20S at failure (ANSYS)	T4L20S at failure (Exp)
		
T5L20S at P=46KN (ANSYS)	T5L20S at failure (ANSYS)	T5L20S at failure (Exp)
		Numerically Investigated only
T2L15S at P=46KN (ANSYS)	T2L15S at failure (ANSYS)	
		
T3L15S at P=46KN (ANSYS)	T3L15S at failure (ANSYS)	T3L15S at failure (Exp)

Figure 19: Cracks Pattern from ANSYS models for the planted cantilever beam at ($P_{max}=46KN$) of the control load and at failure loads with a comparison with the experimental findings.

6.5.2. Numerical load-deflection relationships

The load deflection relationship is constructed for all the investigated specimens and compared with the experimental findings as shown in figures 20 to 24. The graphs showed a very good correlation between the numerical results and the

experimental outcome. Figure 20 for the control specimen showed both curves for the experimental and the analytical are almost similar. In addition, the other graphs showed a little increase in the load and the displacement for the other specimens.

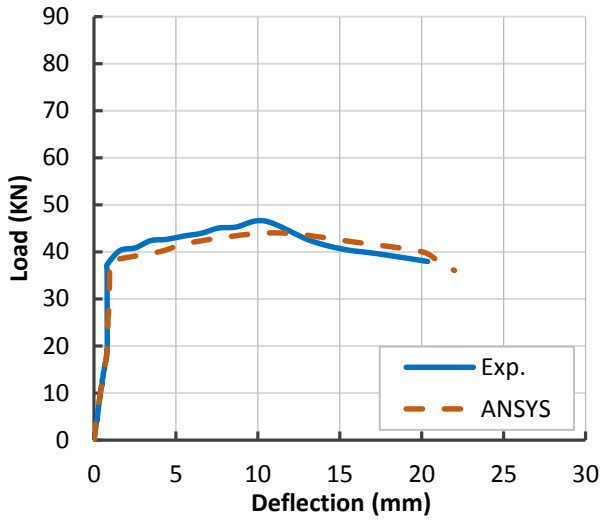


Figure 20: ANSYS and experimental results for the Load-deflection relation of the control specimens

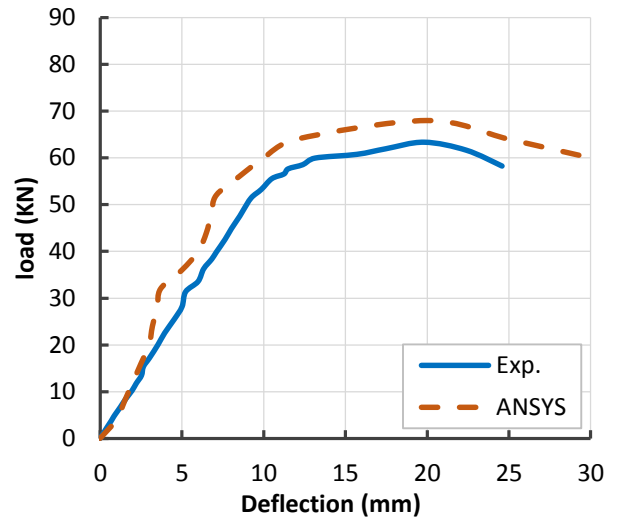


Figure 21: ANSYS and experimental results for the Load-deflection relation of T3L20S specimens

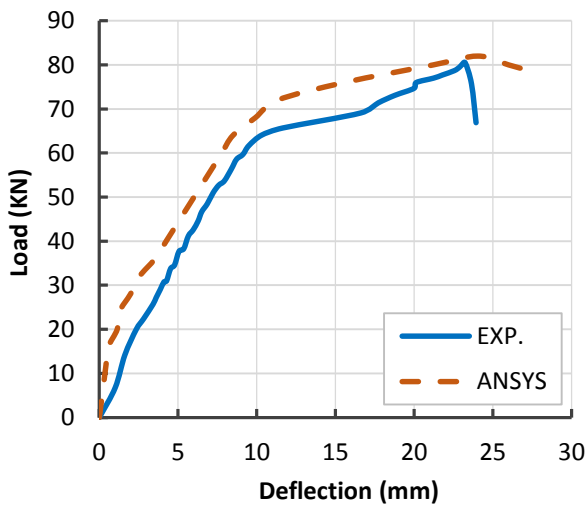


Figure 22: ANSYS and experimental results for the Load-deflection relation of T4L20S specimens

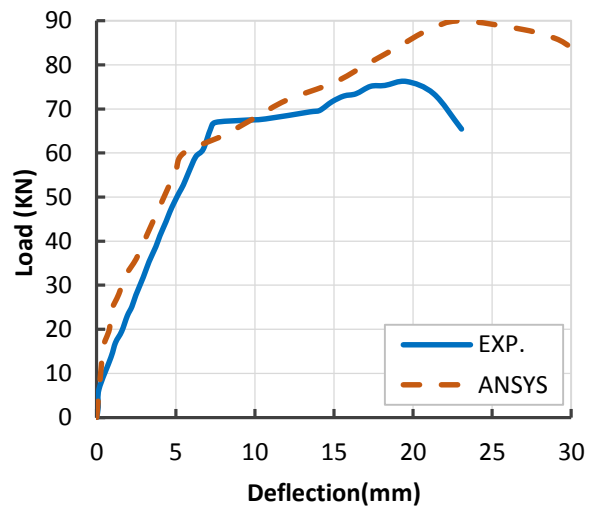


Figure 23: ANSYS and experimental results for the Load-deflection relation of T5L20S specimens

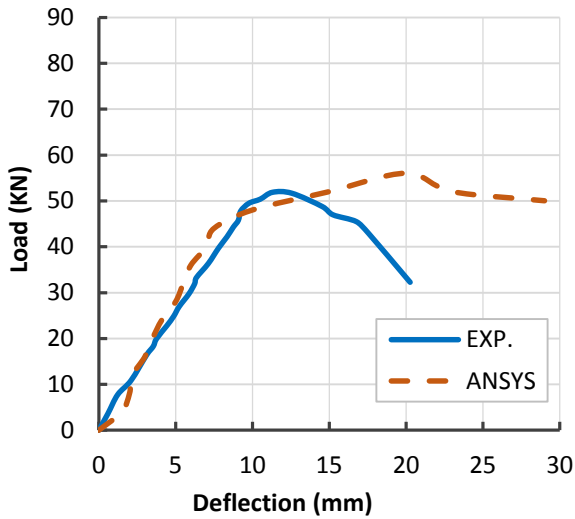


Figure 24: ANSYS and experimental results for the Load-deflection relation of T3L15S specimens

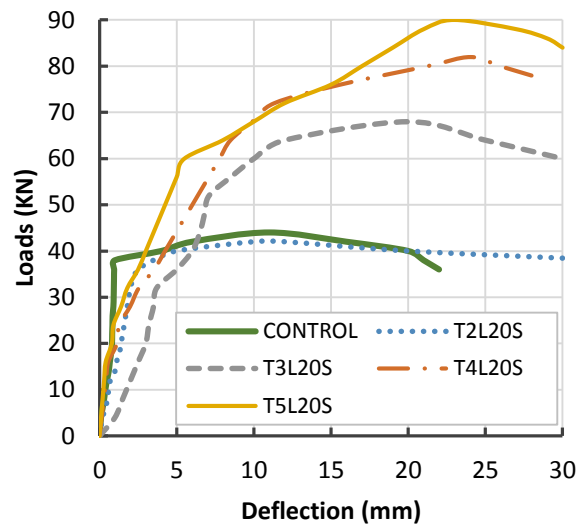


Figure 25: ANSYS and experimental results for the Load-deflection relation of different specimens with the embedment length =20d

The load-deflection relations are presented for all numerically investigated models with the same penetration depth (20d) as shown in figure 25. You may notice that all models achieved the target loads for the control specimen except for T2L20S. All specimens achieved good ductility more than the control specimen. Also, the initial stiffness is close to the stiffness of the control specimens except for T3L20S. You may conclude that using higher reinforcement ratios for planting the bars with depth of 20d achieved the target.

6.5.3. Maximum loads from the numerical models

The maximum loads for each numerical model is presented in the bar chart in figure 26 with the available experimental results. You may find that the values of the numerical and the experimental results are close to each other except for specimen

T5L20S where malfunction problem occurred at the end of the test. Studying those charts, one may find that specimens with a penetration depth of 20d achieved the target load by 95%, 155%, 186%, 200% for planted bars of 2, 3, 4, 5 consequently. Also, specimens with a penetration depth of 15d achieved the target load by 77%, and 127% for planted bars of 2, 3 consequently. Then you must increase the number of the planted bars than for the control specimen.

Moreover, the maximum values for all specimens are presented as a ratio of the control specimen in figure 27 for penetration depths of 15d and 20d. It showed that planting steel bars with the same reinforcement ratio has flexural capacity less than those for the control specimen. So, it is found that the use of planted reinforcement ratio of 150% of those for the control specimen with penetration depths of 15-20d achieved the required strength, stiffness, and ductility.

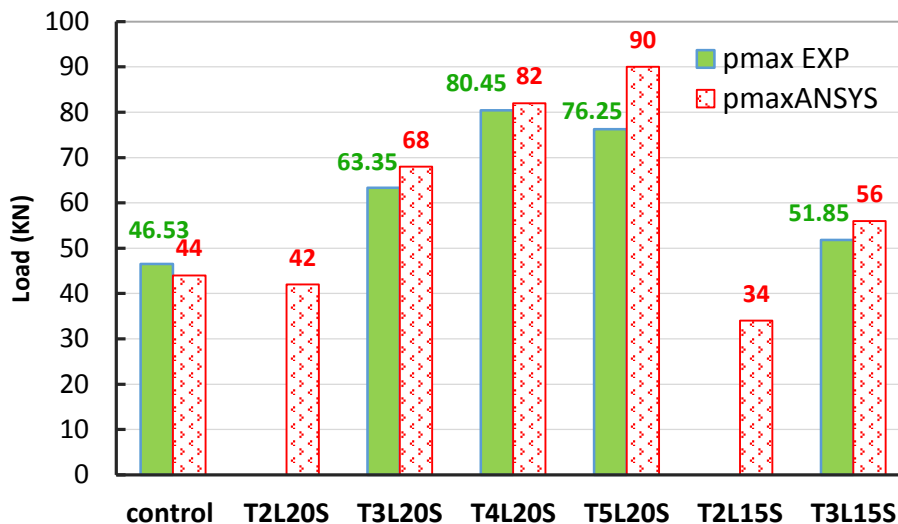


Figure 26: Failure load obtained from the ANSYS and the experimental models

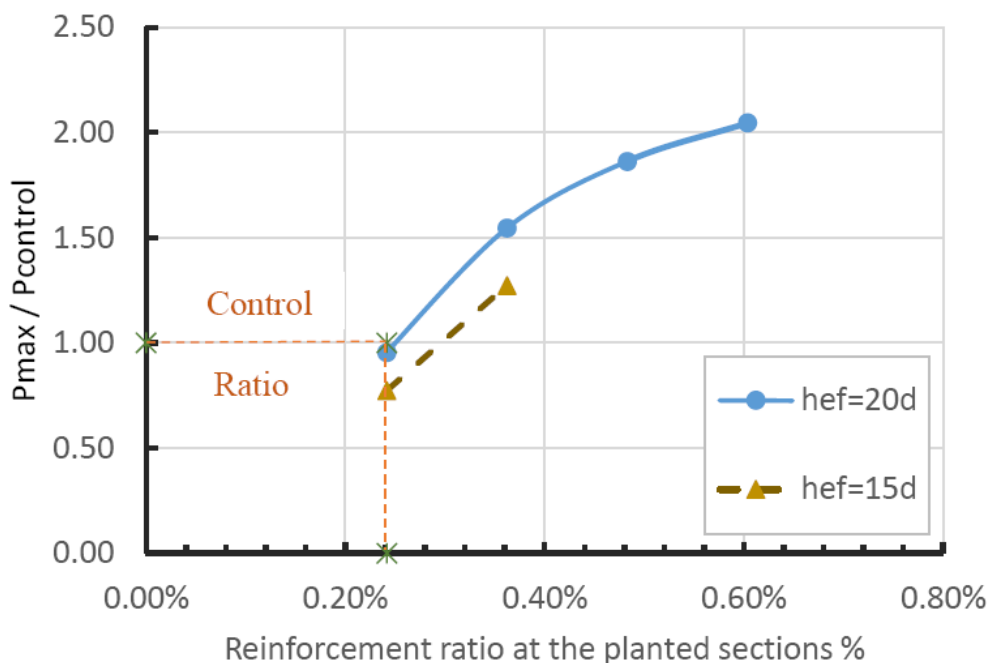


Figure 27: Reinforcement ratio-load capacity relationships for embedment lengths 15d and 20d

7 SUMMARY AND CONCLUSIONS

In stage I: pull out tests are done on planted bars in concrete blocks. The results of such test is evaluated experimentally and numerically. In addition, the findings are compared with the ACI 318-14 equations. The results are analyzed and conclusions are found as:

- The bar diameter does not have a significant effect on the tensile capacity of the planted steel bars since all specimens suffered concrete breakout failure.
- The experimental results are found to be in good agreement with the ACI equations and the numerical findings. More specimens are evaluated using the numerical models only which measured more parameters like another penetration depth and different locations for the restraint part at the top surfaces of the specimens. It is found that using different fixation for the specimens has a great effect on the output results.
- One must use penetration depth of 12d or more to achieve the required pull out capacity of the pulled bars (for the control specimen).
- Mode of failure of the planted steel bars subjected to axial loads or both shear and axial loads is almost concrete breakout failure.

In stage II: the performance of planting a reinforced concrete cantilever on existing concrete columns is investigated experimentally and numerically. The results are analyzed and concluded as follow:

- The experimental results are found to be in good agreement with the numerical findings. Additional specimens are evaluated using the numerical models

only which considered another reinforcement ratio and penetration depth.

- It was found that increasing of the embedment length of the planted steel bars from 15d to 20d has a great effect on the flexural capacity of the planted cantilever beams but does not have an effect on the cracking load.
- Increasing the reinforcement ratio does not change the cracking load. But the failure loads, and the ductility are increased for such specimens with the same embedment length. Also, it caused increase the strain in tensile planted steel bars with a small rate at the same loading.
- The cracks pattern obtained from the numerical models are similar to those obtained from the experimental findings. The spread of the cracks is decreased with increasing of the planting bars ratios when evaluated at the target load (maximum load for the control specimen)
- According to ANSYS results, using planted bars with the same reinforcement ratio as used in the control specimen and embedment length of 20d does not achieve the target loads by (- 4.5%). Also, a similar specimen with embedment length of 15 d failed to achieve the target loads by (- 22.7%). So, it is recommended to use reinforcement ratio more than those for the control specimen.
- You may conclude that using planted bars with double the reinforcement ratio of the control specimen and embedment length of 20 d efficiently achieves the required flexural capacity by an increase of (+87%). Also, the stiffness, deflection, and ductility are efficiently satisfied.

8 REFERENCES

- [1] ACI318-14. Building code requirements for reinforced concrete. Detroit (USA): American Concrete Institute; 2014.
- [2] Blaz Zoubek, Matej Fischinger, and Tatjana Isakovic. (2014) "Estimation of the cycle capacity of beam-to-column dowel connections in precast industrial buildings.
- [3] Çolak, A. (2007). "Estimation of Ultimate Tension Load of Methylmethacrylate Bonded Steel Rods into Concrete." *International Journal of Adhesion and Adhesives*, 27(8), pp. 653-660.
- [4] Cook, R.A. and Konz, R.C. (2001). "Factors Influencing Bond Strength of Adhesive Anchors." *ACI Structural Journal*, 98(1), pp. 76-86.
- [5] Eligehausen, R., Mallee, R., and Silva, J.F. (2006b). *Anchorage in Concrete Construction*, Ernst & Sohn, Berlin, Germany, pp. 186.
- [6] FDOT (2007). *Standard Specifications for Road and Bridge Construction*, Florida Department of Transportation, Tallahassee, FL.
- [7] Krishnamurthy, K. (1996). "Development of a Viscoplastic Consistent-Tangent FEM Model with Applications to Adhesive-Bonded Anchors." Ph.D. dissertation, University of Florida, Gainesville, FL.
- [8] Siamak Epackachi, Omid Esmaili (2015). "Behaviour of adhesive bonded anchors under tension and shear loadings." *Journal of Constructional Steel Research* 114 (2015) 269–280.
- [9] ACI 355.4-11 (2011b). *Qualification of Post-Installed Adhesive Anchors*, American Concrete International, Farmington Hills, MI.
- [10] Adams, R.D. and Wake, W.C. (1984). *Structural Adhesive Joints in Engineering*, Elsevier Applied Science Publishers, London and New York, pp. 160-162.
- [11] ASTM C881/C881M (2002). *Standard Specification for Epoxy Resin-Base Bonding Systems for Concrete*, American Society for Testing and Materials, West Conshohocken.
- [12] Caldwell, D. (2001). *Surface Chemical Analysis of Aggregate*, Polymer Solutions Incorporated, Blacksburg, VA.